Science Advances
AAAS

Supplementary Materials for

Activated I-BAR IRSp53 clustering controls the formation of VASP-actin–based membrane protrusions

Feng-Ching Tsai *et al.*

Corresponding author: Feng-Ching Tsai, feng-ching.tsai@curie.fr; Gregory A. Voth, gavoth@uchicago.edu; Pekka Lappalainen, pekka.lappalainen@helsinki.fi; Patricia Bassereau, patricia.bassereau@curie.fr

Sci. Adv. **8**, eabp8677 (2022)
DOI: 10.1126/sciadv.abp8677

The PDF file includes:

Figs. S1 to S19
Legends for movies S1 to S11

Other Supplementary Material for this manuscript includes the following:

Movies S1 to S11

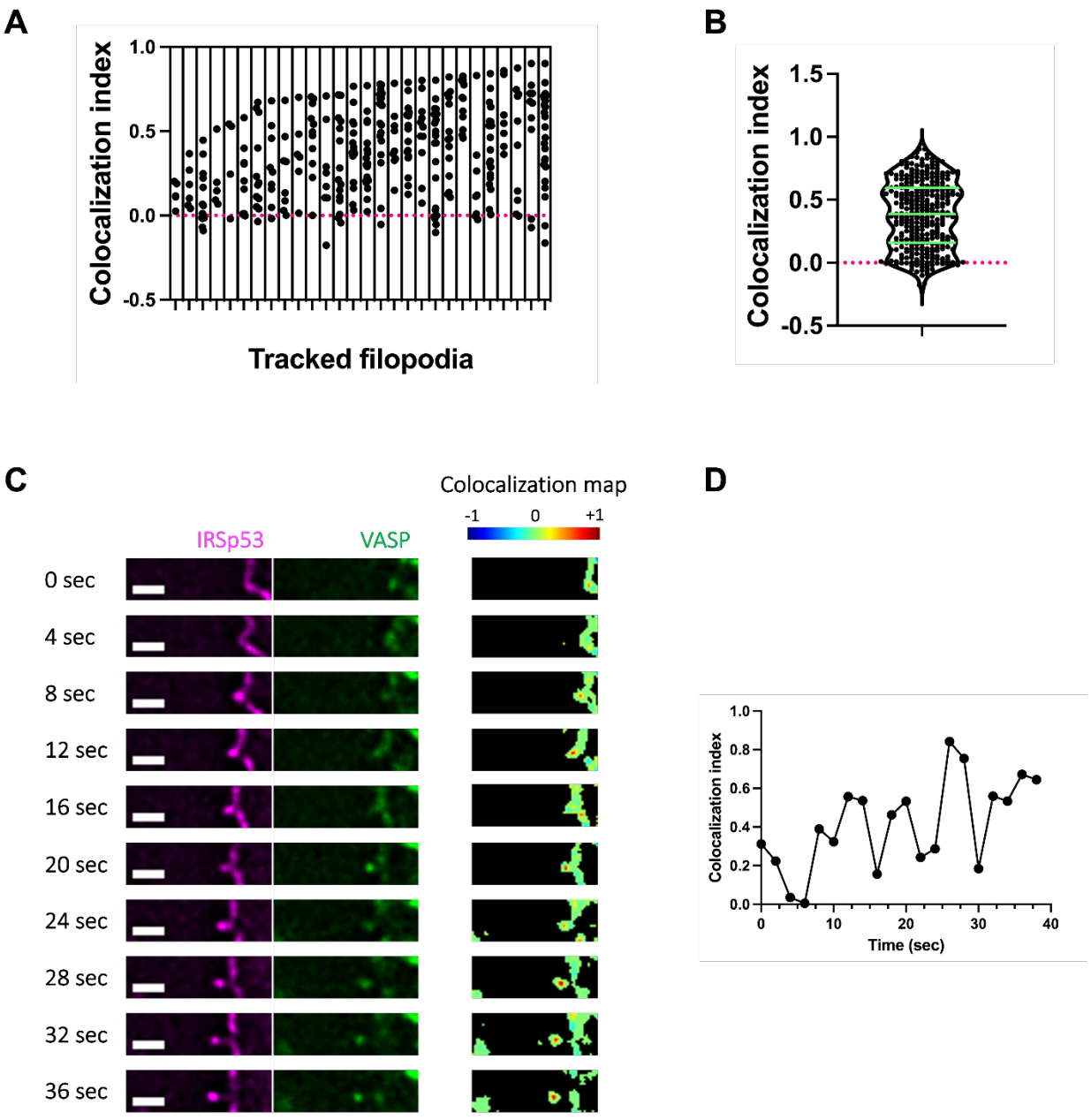

Fig. S1. Colocalization of IRSp53 and VASP during filopodia formation

(A) Colocalization indexes of tracked filopodia. Each individual column shows the indexes of an individually tracked filopodium; inside each column, data points correspond to the colocalization indexes measured at different time points. N = 28 filopodia, n = 2 experiments. Red dotted line indicates 0 value. (B) Violin plot of all the colocalization indexes of the 28 tracked filopodia. Quartiles and median are shown as green lines. Red dotted line indicates 0 value. (C) *Left panel*. Time-lapse widefield fluorescence images of a representative tracked filopodium in a Rat2 cell transfected with IRSp53-eGFP and RFP-VASP. Color codes: magenta, IRSp53-eGFP and green, RFP-VASP. Scale bars, 1 μm. *Right panel*. Color-coded colocalization maps of the tracked filopodium shown on the *Left*. Color maps: low colocalization index in blue, and high

colocalization index in red. (D) Colocalization indexes during the formation of the filopodium shown in (C).

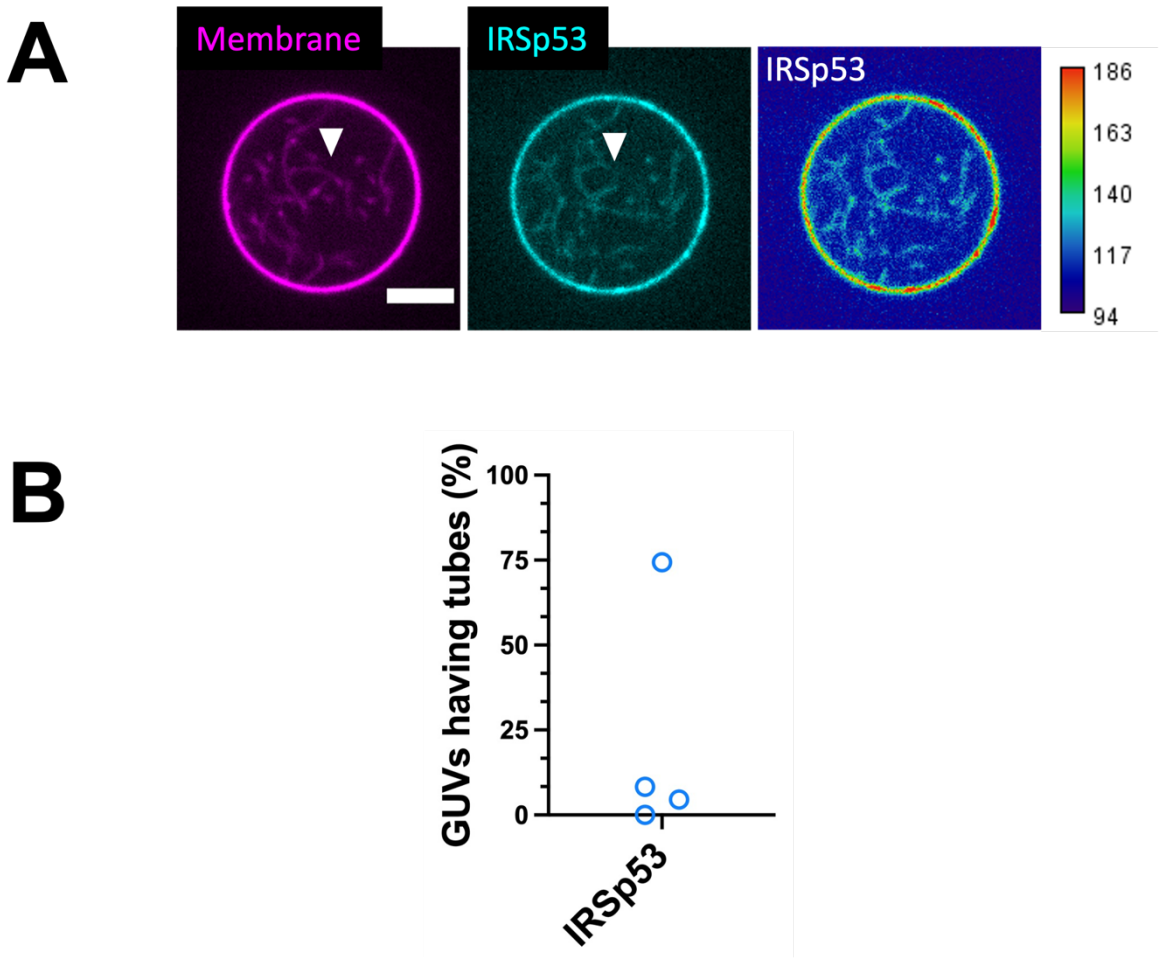

Fig. S2. IRSp53 generates inward membrane tubes on GUVs.

(A) Representative confocal images of GUVs incubated with AX488 labelled IRSp53 (16 nM, dimer). Color codes: magenta, membrane and cyan, IRSp53. Heat map: high IRSp53 intensity in red and low intensity in blue. White arrowhead indicates some membrane tubes. GUV membrane composition: TBX supplemented with 0.5% TR-ceramide and 5% PIP_2. Scale bar, 5 μm. (B) Percentages of GUVs having tubes generated by AX488 labelled IRSp53 (16 nM, dimer). N = 22, 24, 43, 15 GUVs, n = 4 sample preparations.

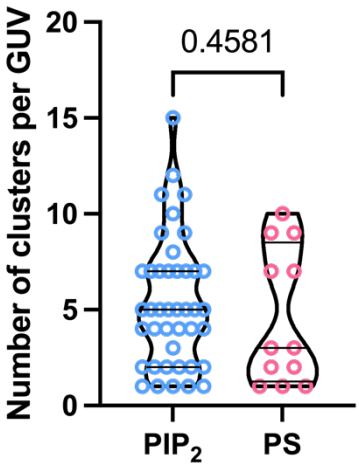

Fig. S3. Comparable numbers of IRSp53 clusters on PIP_2-GUVs and PS-GUVs.
Characterization of the numbers of IRSp53 clusters on PIP_2-GUVs ("PIP_2") and PS-GUVs ("PS"). "PIP_2", N = 225 clusters from 58 GUVs, n = 3 sample preparations. "PS", N = 55 clusters from 20 GUVs, n = 2 sample preparations. Statistical test: two-tailed Mann-Whitney test, $p = 0.4581$.

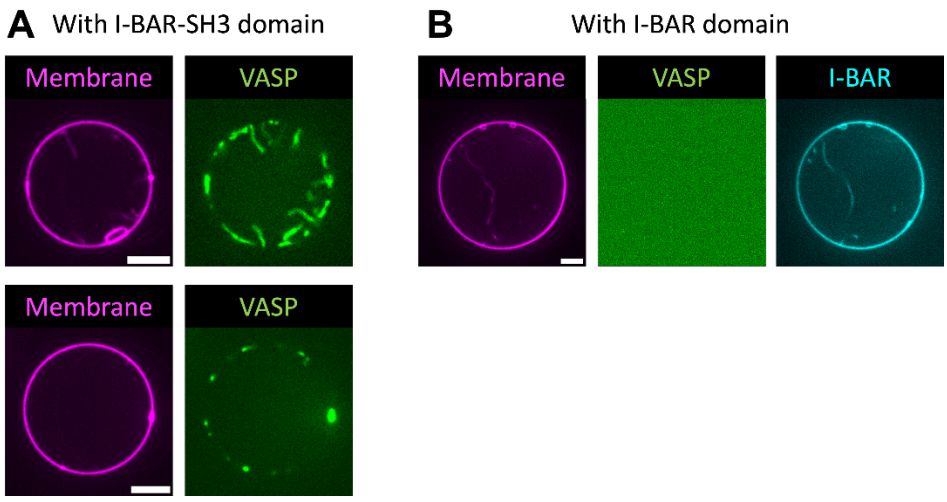

Fig. S4. The I-BAR-SH3 domain of IRSp53 but not the I-BAR domain of IRSp53 recruits VASP to GUV membranes.

(A and B) Representative confocal images of GUVs incubated with AX488-labelled VASP in the presence of non-fluorescently labelled I-BAR-SH3 domain of IRSp53 (A) or the I-BAR domain of IRSp53 (B). Membrane composition: TBX supplemented with 0.5% TR-ceramide and 5% PIP_2. Protein concentration: unlabeled I-BAR-SH3 domain (16 nM, dimer), AX647-labeled I-BAR domain (16 nM, dimer), and AX488-labelled VASP (4 nM tetramer). Scale bars: 5 μm.

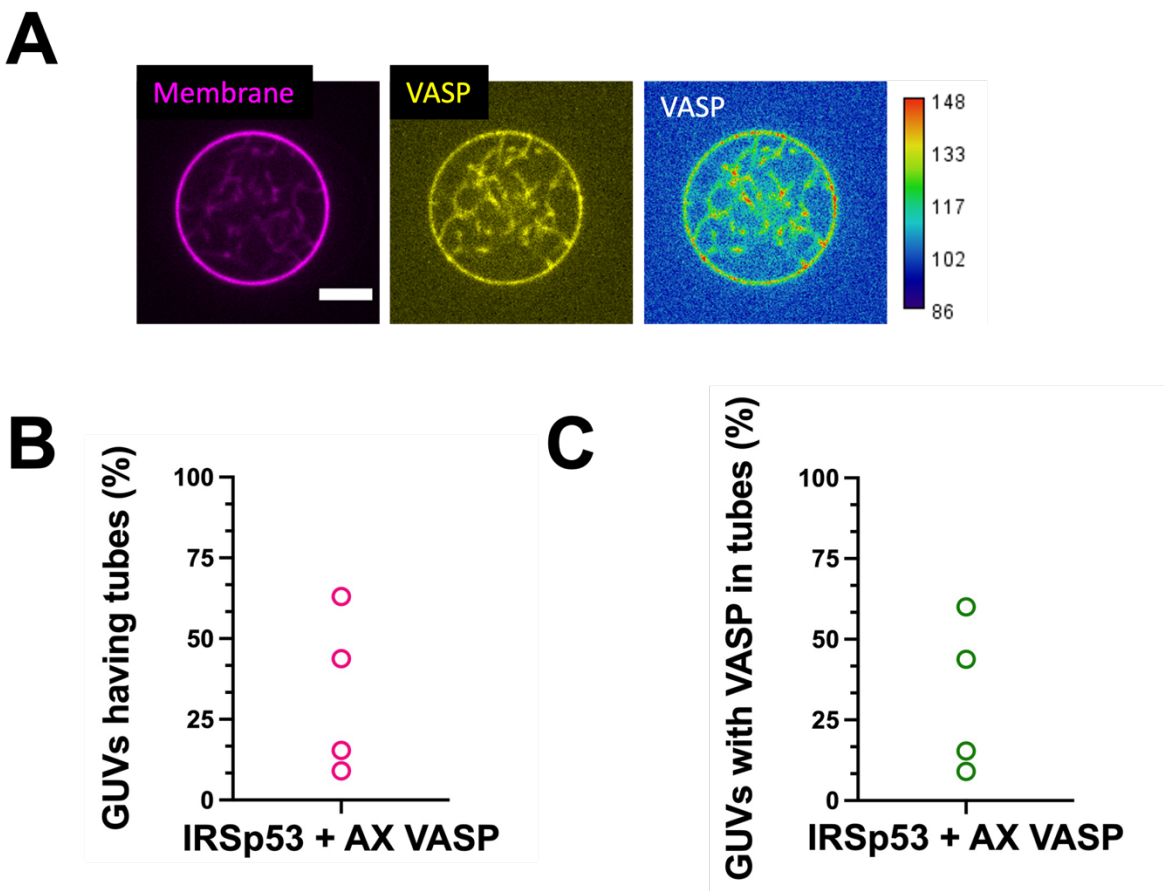

Fig. S5. VASP is recruited to IRSp53 generated membrane tubes on GUVs.

(A) Representative confocal images of GUVs incubated with IRSp53 (unlabeled, 16 nM dimer) and AX488-labelled VASP (4 nM tetramer). Color codes: magenta, membrane and yellow, VASP. Heat map: high VASP intensity in red and low intensity in blue. Scale bar, 5 µm. (B) Percentages of GUVs having tubes in the presence of unlabeled IRSp53 (16 nM, dimer) and AX488-labelled VASP (4 nM, tetramer). N = 16, 13, 43, 11 GUVs, n = 4 sample preparations. (C) Percentages of GUVs having VASP-positive tubes in the presence of unlabeled IRSp53 (16 nM, dimer) and AX488-labelled VASP (4 nM tetramer). N = 16, 13, 43, 11 GUVs, n = 4 sample preparations. GUV membrane composition: TBX supplemented with 0.5% TR-ceramide and 5% PIP_2.

A

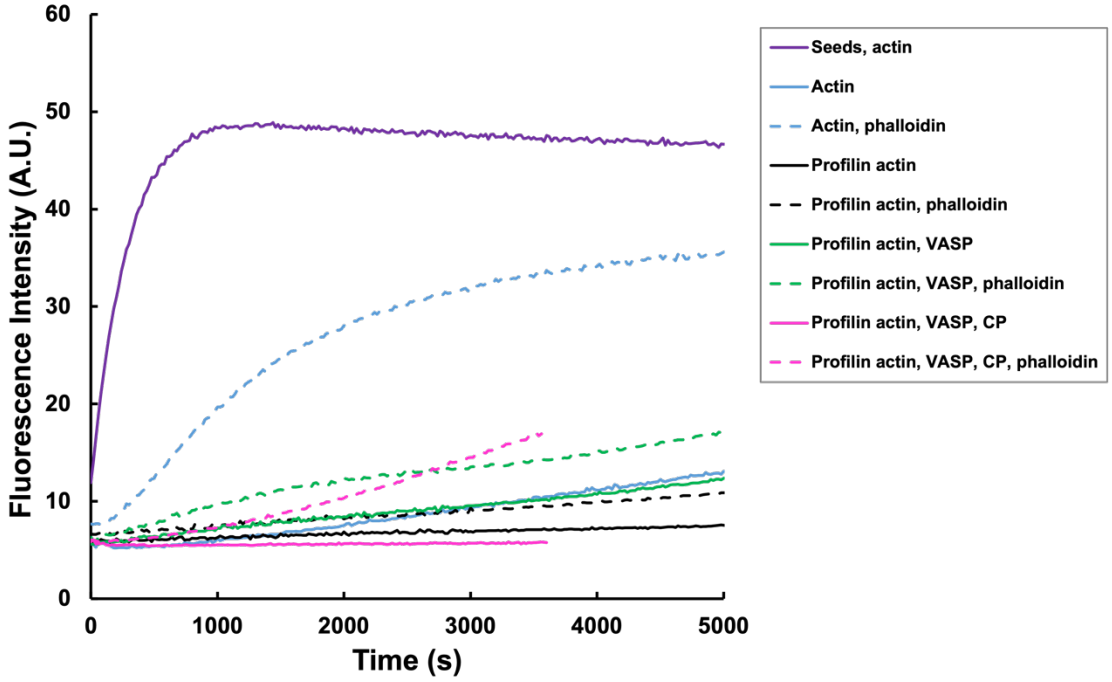
Fluorescence Intensity (A.U.)
Time (s)
0
10
20
30
40
50
60
0
1000
2000
3000
4000
5000
Seeds, actin
Actin
Actin, phalloidin
Profilin actin
Profilin actin, phalloidin
Profilin actin, VASP
Profilin actin, VASP, phalloidin
Profilin actin, VASP, CP
Profilin actin, VASP, CP, phalloidin

B

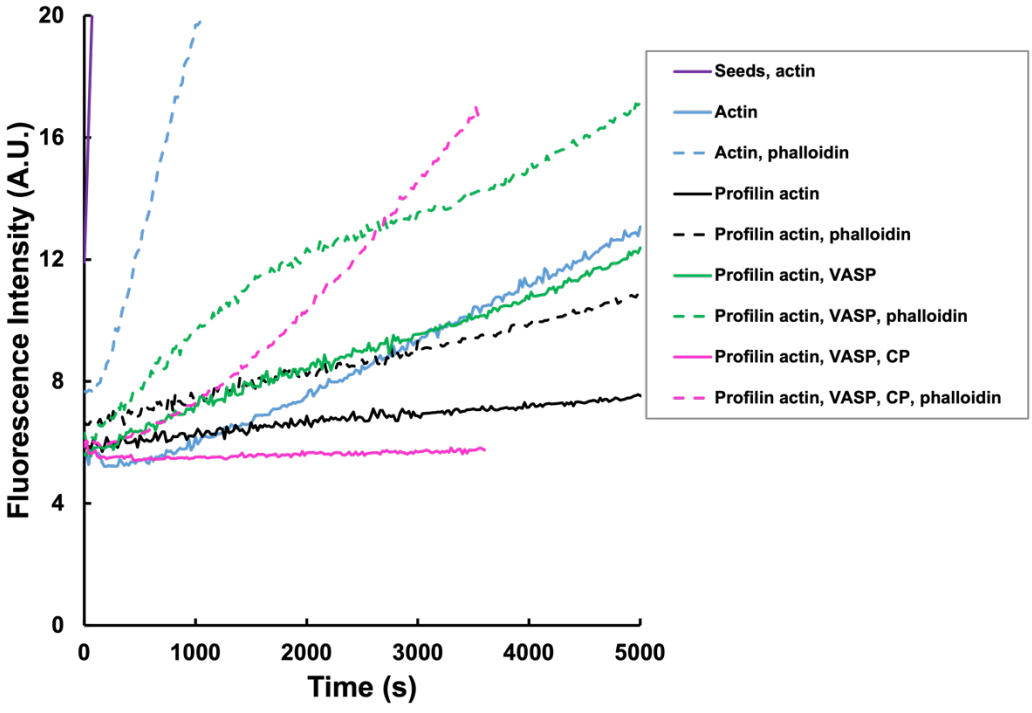
Fluorescence Intensity (A.U.)
Time (s)
0
4
8
12
16
20
0
1000
2000
3000
4000
5000
Seeds, actin
Actin
Actin, phalloidin
Profilin actin
Profilin actin, phalloidin
Profilin actin, VASP
Profilin actin, VASP, phalloidin
Profilin actin, VASP, CP
Profilin actin, VASP, CP, phalloidin

Fig. S6. Effects of VASP, capping protein (CP) and phalloidin in profilin-actin polymerization in bulk.

(A and B) Pyrene actin polymerization assay. Actin (2 μM, 5% pyrenyl labeled) was spontaneously assembled with, if present, spectrin-actin seeds, named seeds (0.2 nM), profilin (2.4 μM), VASP (15 nM in tetramer), CP (25 nM) and phalloidin (2 μM) (color coded). (B) Zoomed-in of data shown in (A).

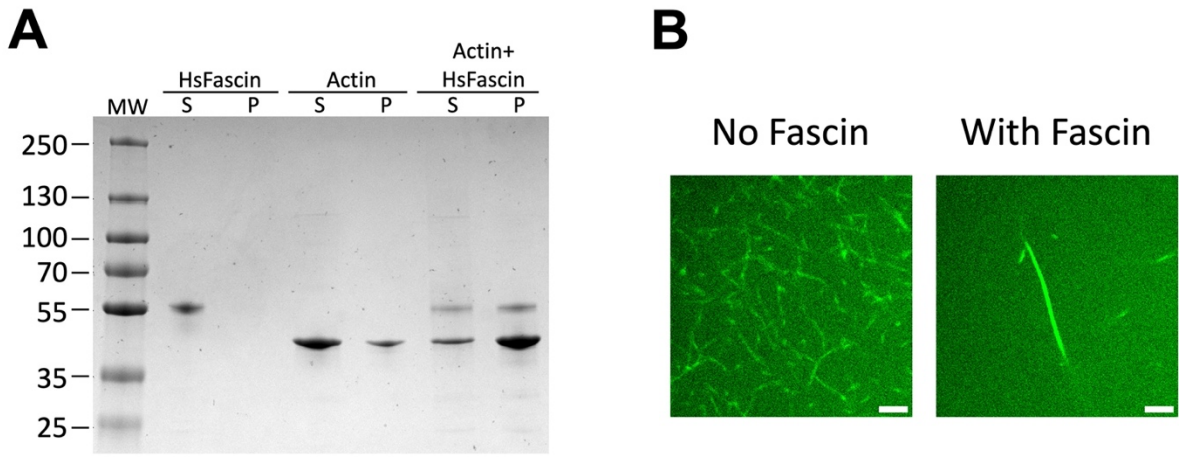

Fig. S7. Purified fascin can bundle actin filaments.

(A) Actin co-sedimentation assay. Commassie stained SDS-PAGE gel containing supernatant (S) and pellet (P) fractions after low-speed centrifugation (19,000 rpm) of recombinantly produced HsFascin, filamentous non-muscle actin, and the mixture of HsFascin and filamentous non-muscle actin. (B) Representative confocal images of filamentous muscle actin visualized by AX488 phalloidin in the absence (*Left*) and presence (*Right*) of fascin. Scale bars: 5 μm.

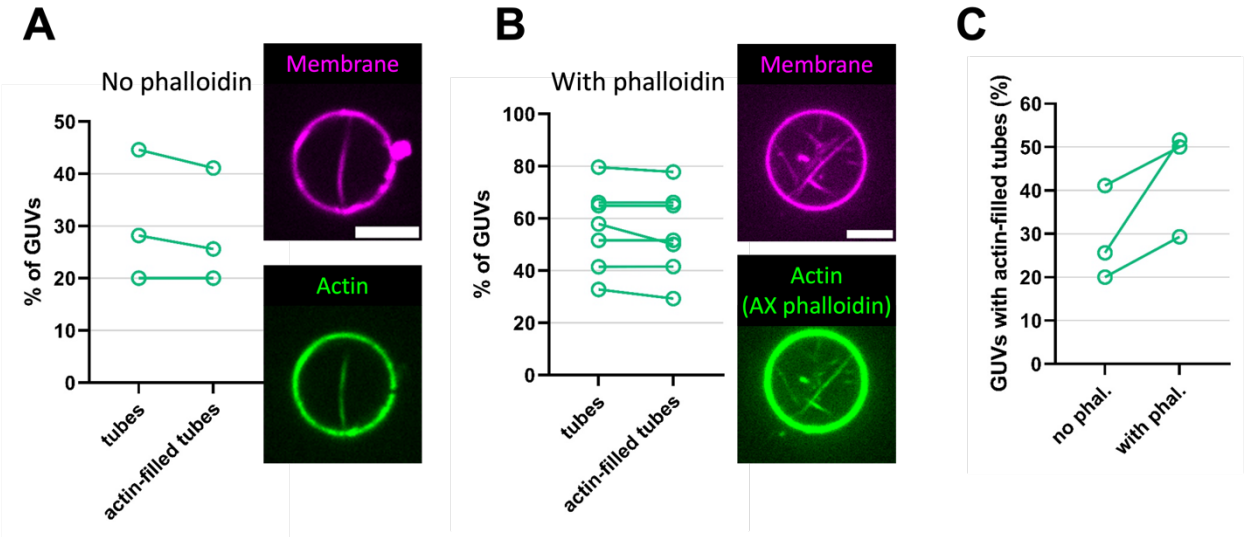

Fig. S8. Quantifications of GUVs with actin-filled tubes in the presence and absence of phalloidin.

(A and B) *Left* panel. Percentages of GUVs with membrane tubes ("tubes") and with at least one or more actin-filled tubes ("actin-filled tubes"), (A) in the absence ("No phalloidin") and (B) in the presence ("With phalloidin") of AX488 phalloidin. For "No phalloidin" condition, AX488 labelled actin was used. Total GUV numbers: "No phalloidin", 56, 39, 45; "With phalloidin", 57, 56, 41, 54, 58, 62, 38. *Right* panel. Representative confocal images of GUVs with actin-filled tubes. Actin was visualized by AX488 labelled actin (10%-27% AX488 labelled) (A) or by AX488 phalloidin (B). GUVs (shown in magenta) were composed of TBX supplemented with 0.5% TR-ceramide and 5% PIP_2. GUVs were incubated with IRSp53 (16 nM dimer), VASP (4 nM tetramer), actin (0.5 μM, shown in green), fascin (250 nM), capping proteins (25 nM) and profilin (0.6 μM). Scale bars: 5 μm. (C) Total GUV numbers: In the absence of phalloidin, "no phal.", 56, 39, 45; in the presence of phalloidin, "with phal.", 38, 62, 58.

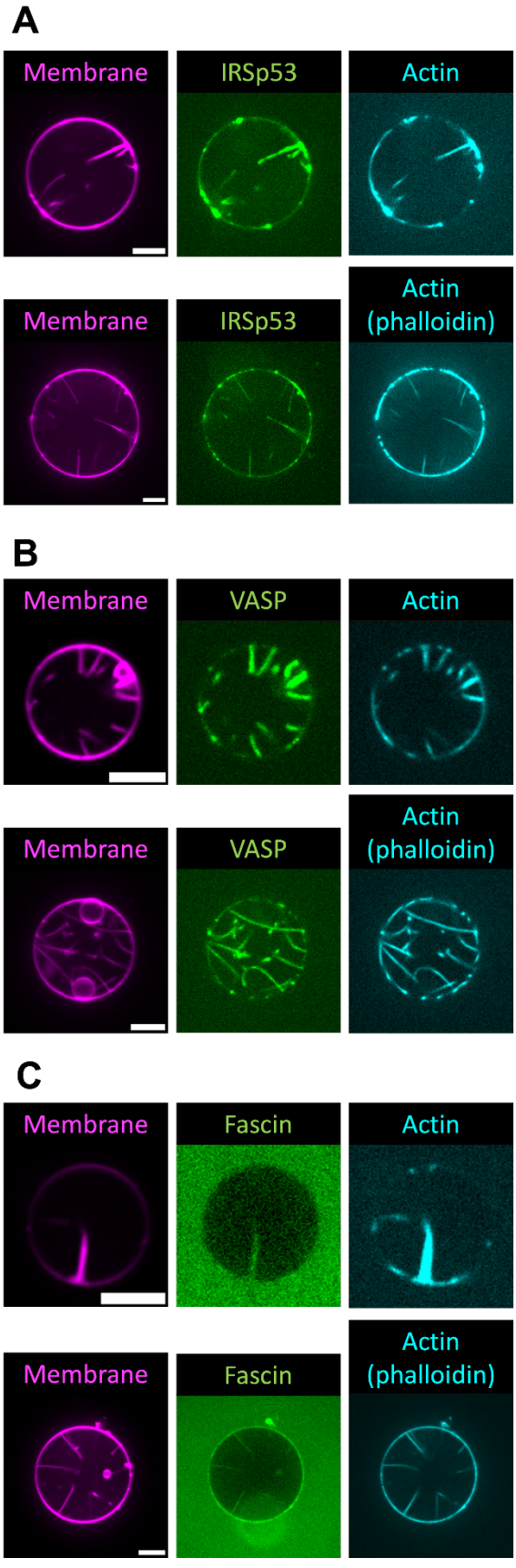
A
Membrane
IRSp53
Actin
Membrane
IRSp53
Actin
(phalloidin)
B
Membrane
VASP
Actin
Membrane
VASP
Actin
(phalloidin)
C
Membrane
Fascin
Actin
Membrane
Fascin
Actin
(phalloidin)

Fig. S9. Localization of IRSp53, VASP and fascin in actin-filled membrane protrusions.

(A-C) Representative confocal images of GUVs with actin-filled membrane protrusions. To visualize membranes, Cy5-PC is included in the lipid mixtures. To visualize actin, AX594-actin (Top Panels) or AX594-phalloidin (Bottom Panels) was used. To visualize IRSp53, VASP or fascin in membrane tubes, we used AX488-labelled IRSp53 (A), AX488-labelled VASP (B) or AX488-labelled fascin (C). Membrane composition: TBX supplemented with 0.5% Cy5-PC and 5% PIP_2. Protein concentration: IRSp53 (16 nM dimer), VASP (4 nM tetramer), actin (0.5 μM), fascin (250 nM), capping proteins (25 nM) and profilin (0.6 μM). Scale bars, 5 μm.

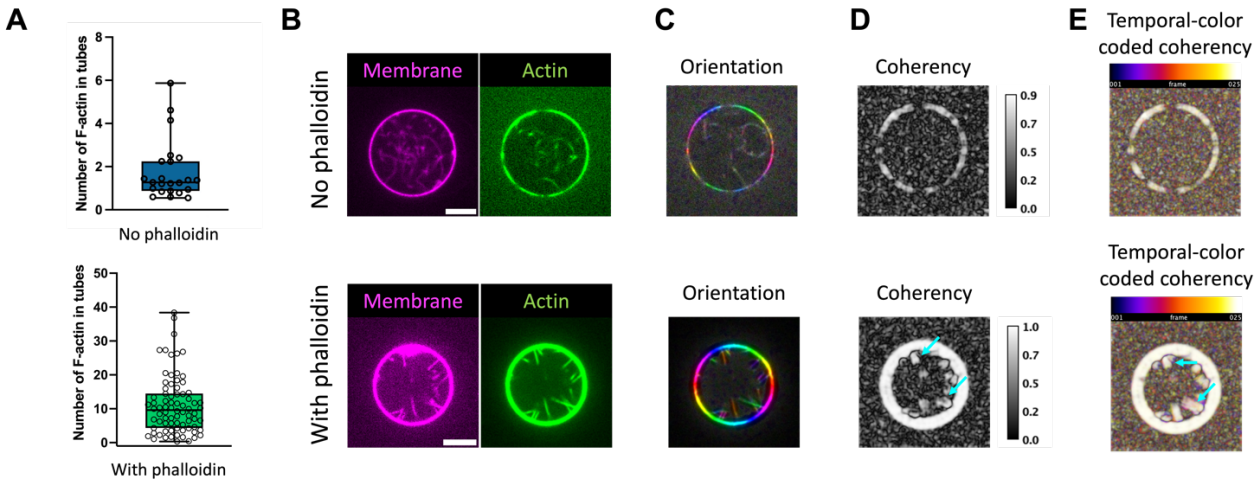

Fig. S10. Quantifications of the number of filamentous actin (F-actin) and the orientational properties of the actin-filled membrane tubes in the presence and absence of phalloidin.

Top panel, in the absence of phalloidin and *Bottom* panel, in the presence of phalloidin. (A) Numbers of filamentous actin (F-actin) in tubes. In the presence of phalloidin, N = 78 tubes, n = 3 sample preparations. In the absence of phalloidin: N = 23 tubes, n = 1 sample preparation. (B) Representative confocal images of GUVs with actin-filled membrane protrusions. Actin was visualized by AX488-labelled actin (*Top panel*) or by AX488 phalloidin (*Bottom Panel*). Scale bars: 5 μm. (C) Color-coded local orientational properties of the corresponding actin images shown in (B). The images were generated using the HSB mode, H: hue, corresponds to the orientation; S: saturation to the coherency; B: brightness of the source image. (D) *Left*. Coherency map of the corresponding actin images shown in (B). *Right*. Color-coded bars indicate the values of coherency indexes in the corresponding coherency maps shown in the *Left*. Cyan arrows indicate places where the actin-filled tubes are. (E) Temporal-color coded coherency maps of 25 sequential confocal images of actin of the corresponding GUVs shown in (B). Cyan arrows indicate places where the actin-filled tubes are. The color-coded bars on the top of the images indicate the frame number from 1 to 25. The images are from Movie S4 and Movie S7.

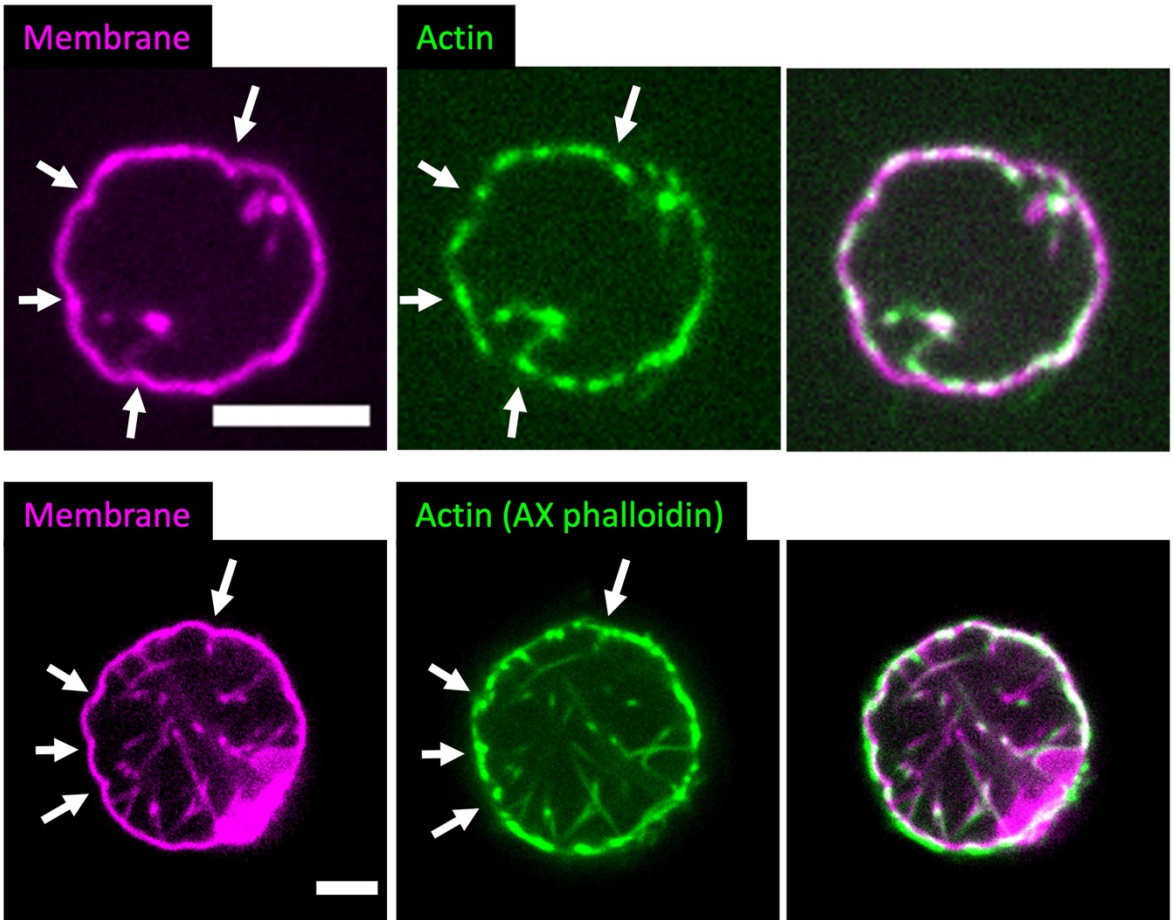

Fig. S11. Membrane deformation by the IRSp53-VASP-actin networks.

Representative confocal images of GUVs deformed by actin in the absence (*Top* panel) and presence (*Bottom* panel) of phalloidin. Actin was visualized by AX488-labelled actin (*Top* panel) or by AX488 phalloidin (*Bottom* panel). GUV membrane composition: TBX supplemented with 0.5% TR-ceramide and 5% PIP_2. GUVs were incubated with IRSp53 (16 nM dimer), VASP (4 nM tetramer), actin (0.5 μM), fascin (250 nM), capping proteins (25 nM) and profilin (0.6 μM). Color codes: magenta, membranes and green, actin. White arrows indicate some inward membrane deformations on the GUV membranes. Scale bars, 5 μm.

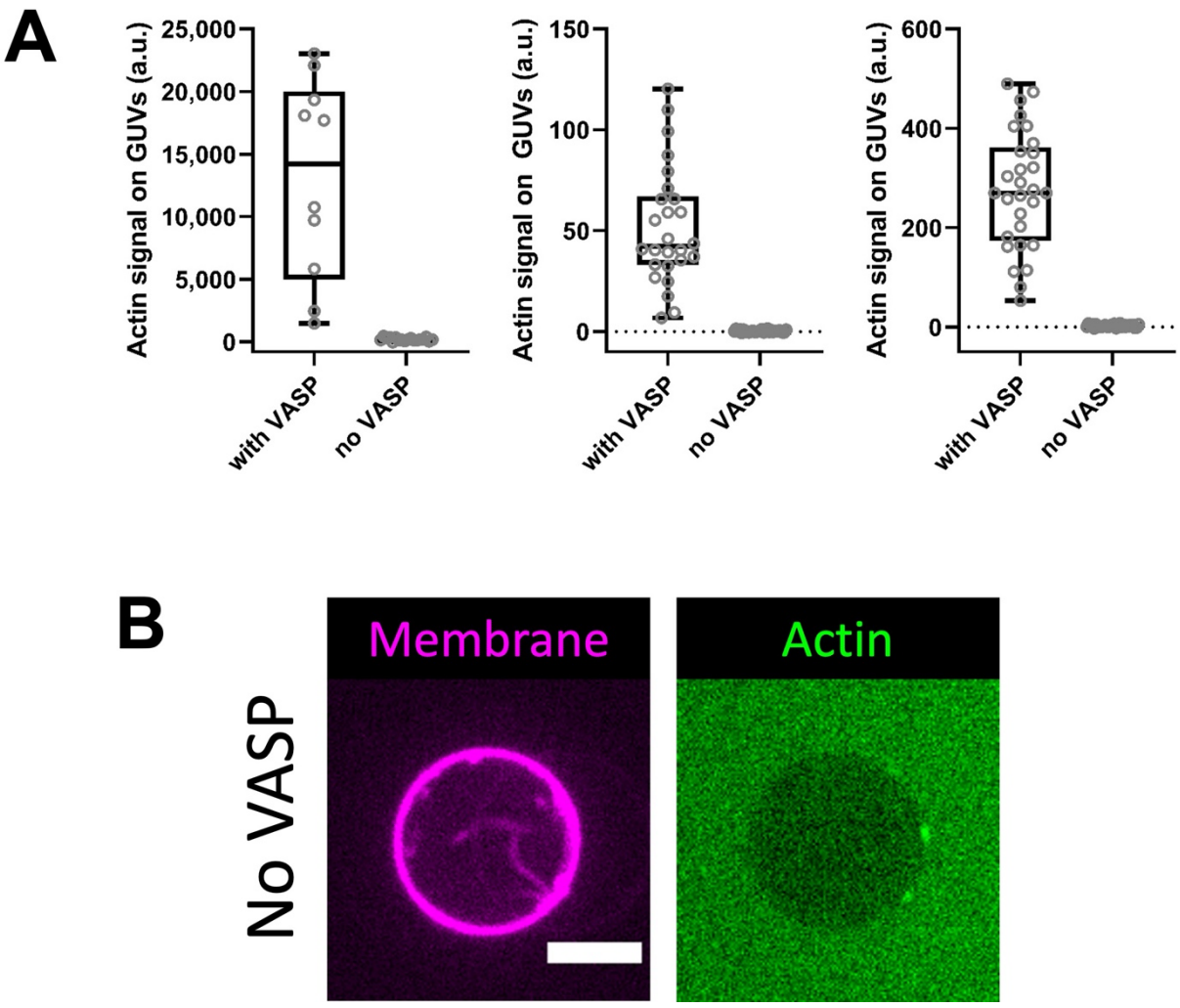

Fig. S12. A complete lack of actin signals on GUVs in the absence of VASP.

(A) The results showed three sample preparations. From left to right. N = 10, 18 GUVs, N = 26, 29 GUVs and N = 29, 29 GUVs, in the presence ("with VASP") and absence ("No VASP") of VASP. (B) Representative confocal images of a GUV having tubes in the absence of VASP. Actin was visualized by AX488-labelled actin. GUV membrane composition: TBX supplemented with 0.5% TR-ceramide and 5% PIP_2. GUVs were incubated with IRSp53 (16 nM dimer), actin (0.5 μM), fascin (250 nM), capping proteins (25 nM) and profilin (0.6 μM). Color codes: magenta, membranes and green, actin. Scale bar, 5 μm.

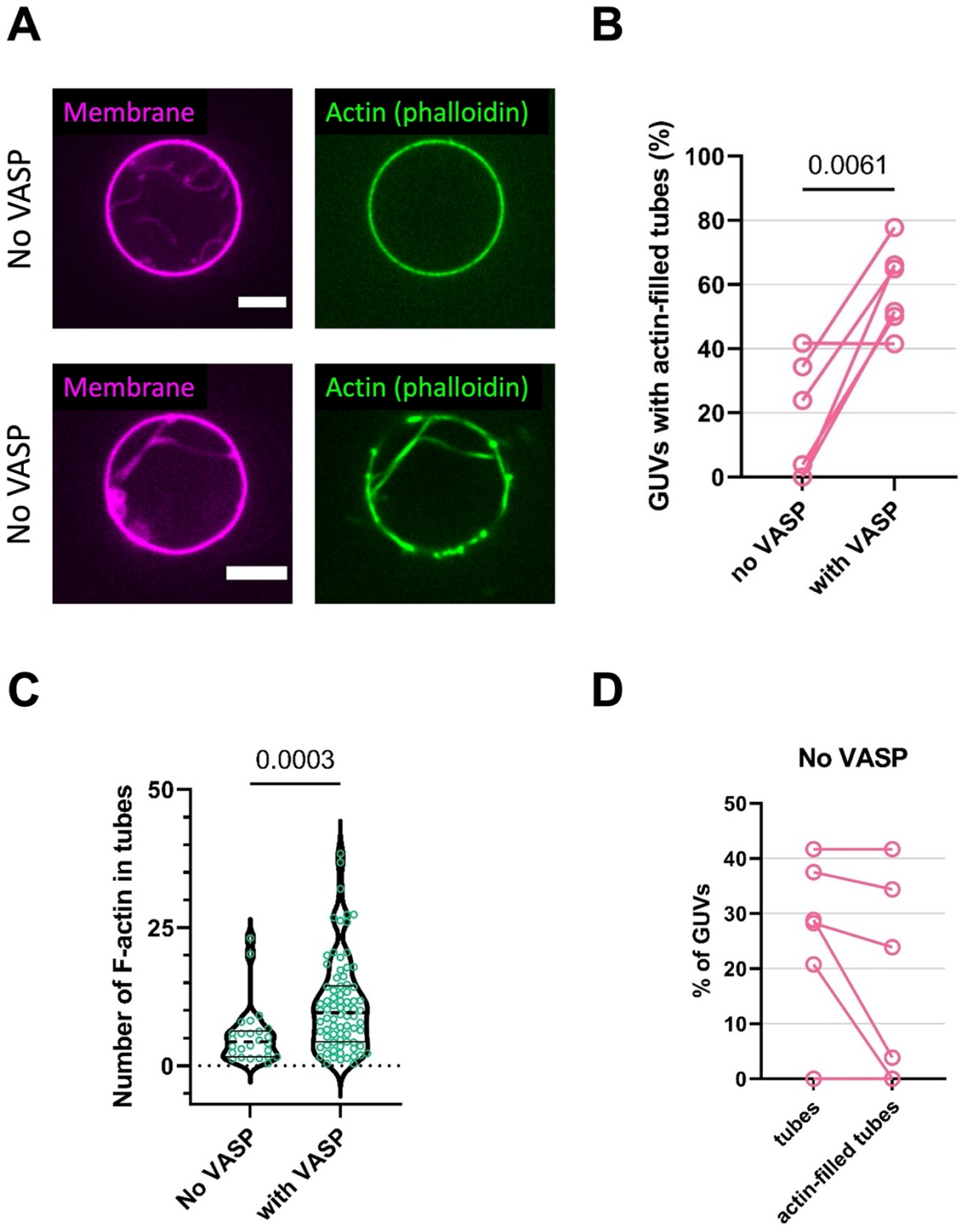

Fig. S13. VASP facilitates protrusion formation by promoting actin polymerization in the presence of phalloidin.

(A) Representative confocal images of GUVs incubated with IRSp53 (16 nM dimer), actin (0.5 μM), fascin (250 nM), capping proteins (25 nM) and profilin (0.6 μM), i.e., in the absence of

VASP. Actin was visualized by AX488 phalloidin. GUV membrane composition: TBX supplemented with 0.5% TR-ceramide and 5% PIP_2. Color codes: magenta, membranes and green, actin. Scale bars, 5 μm. (B) Percentages of GUVs with actin-filled tubes in the absence ("No VASP") and presence ("with VASP") of VASP. "With VASP", N = 41, 54, 57, 38, 56, 62 GUVs and "No VASP", N = 24, 32, 46, 52, 17, 53 GUVs. n = 6 sample preparations. Statistical tests: (1) chi-squared test on data pooled from the 6 sample preparations, $p < 0.0001$, and (2) paired *t* test considering the 6 sample preparations individually, $p = 0.0061$ (shown in the figure). (C) Numbers of filamentous actin (F-actin) inside the tubes in the absence ("No VASP") and presence ("with VASP") of VASP. N = 26 ("No VASP") and 78 ("With VASP") tubes, n = 3 sample preparations. Note that "with VASP" data are the same as shown in Fig. S10 A. Statistical test: Mann-Whitney test, unequal variance, $p = 0.0003$. (D) In the absence of VASP, percentages of GUVs with tubes and actin-filled tubes.

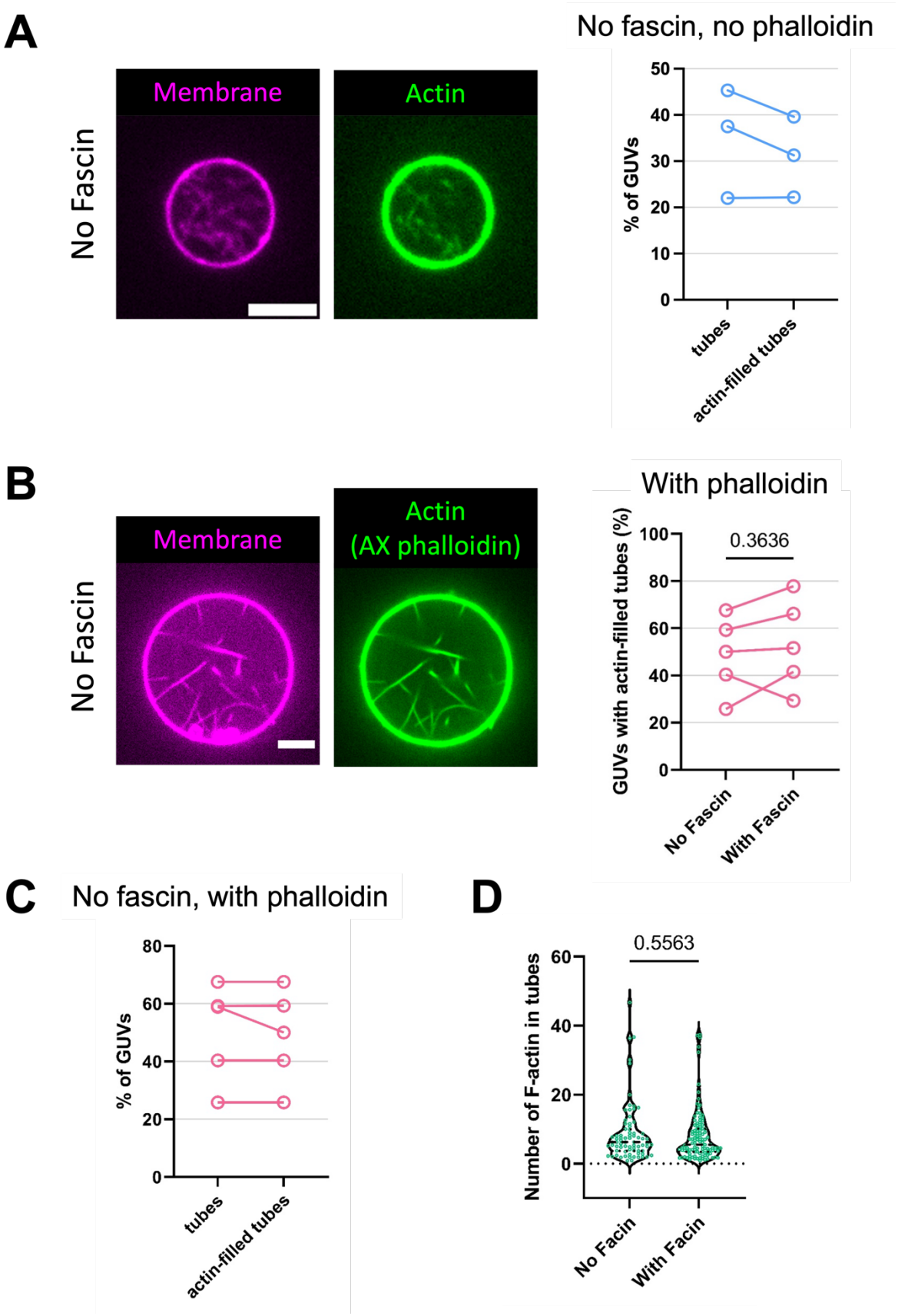
A
No Fascin
Membrane
Actin
No fascin, no phalloidin
% of GUVs
50
40
30
20
10
0
tubes
actin-filled tubes
B
No Fascin
Membrane
Actin
(AX phalloidin)
With phalloidin
GUVs with actin-filled tubes (%)
0.3636
100
80
60
40
20
0
No Fascin
With Fascin
C
No fascin, with phalloidin
% of GUVs
80
60
40
20
0
tubes
actin-filled tubes
D
Number of F-actin in tubes
0.5563
60
40
20
0
No Facin
With Facin

Fig. S14. Fascin does not facilitate IRSp53-based protrusion formation.

(A) *Left* panel, representative confocal images of GUVs incubated with IRSp53 (16 nM dimer), VASP (4 nM tetramer), actin (0.5 μM, with 10% - 27% AX488 actin), capping proteins (25 nM) and profilin (0.6 μM), i.e., in the absence of fascin. GUV membrane composition: TBX supplemented with 0.5% TR-ceramide and 5% PIP_2. Color codes: magenta, membranes and green, actin. Scale bar, 5 μm. *Right* panel, in the absence of fascin and phalloidin, percentages of GUVs with membrane tubes ("tubes") and with at least one or more actin-filled tubes ("actin-filled tubes"). GUV numbers, N = 32, 54, 53, n = 3 sample preparations. (B – D) In the presence of AX488 phalloidin, (B) *Left* panel, representative confocal images of GUVs incubated with IRSp53 (16 nM dimer), actin (0.5 μM), VASP (4 nM tetramer), capping proteins (25 nM), profilin (0.6 μM), and AX488 phalloidin, i.e., in the absence of fascin. GUV membranes were visualized by including 0.5 mol% BODIPY TR ceramide in the lipid mixture. Scale bar, 5 μm. *Right* panel, percentages of GUVs with actin-filled tubes in the absence ("No Fascin") and presence ("With Fascin") of fascin. "With Fascin", N = 54, 56, 62, 58, 41 GUVs and "No Fascin", N = 37, 54, 56, 57, 31 GUVs. n = 5 sample preparations. Statistical tests: (1) chi-squared test on data pooled from the 5 sample preparations, $p = 0.3522$, and (2) paired *t* test considering the 5 sample preparations individually, $p = 0.3636$ (shown in the figure). (C) In the absence of fascin, percentages of GUVs with membrane tubes ("tubes") and with at least one or more actin-filled tubes ("actin-filled tubes"). N = 37, 54, 56, 57, 31 GUVs, n = 5 sample preparations. (D) Numbers of F-actin inside the tubes in the absence ("No Fascin") and presence ("With Fascin") of Fascin. N = 76 ("No Fascin") and 109 ("With Fascin") tubes, n = 3 sample preparations. Statistical test: Unpaired *t* test, $p = 0.5563$.

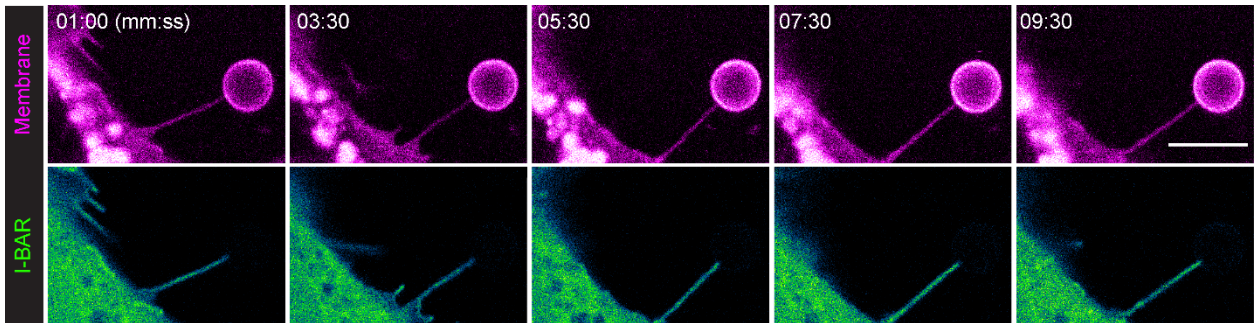

Fig. S15. IRSp53's I-BAR domain is visibly present in nanotubes shortly after pulling. Selected still images from Movie S9. Color codes: Cell Mask™ Deep Red (magenta), I-BAR-eGFP (green). Imaging started 1 minute after the nanotube was formed. Scale bar, 5 µm.

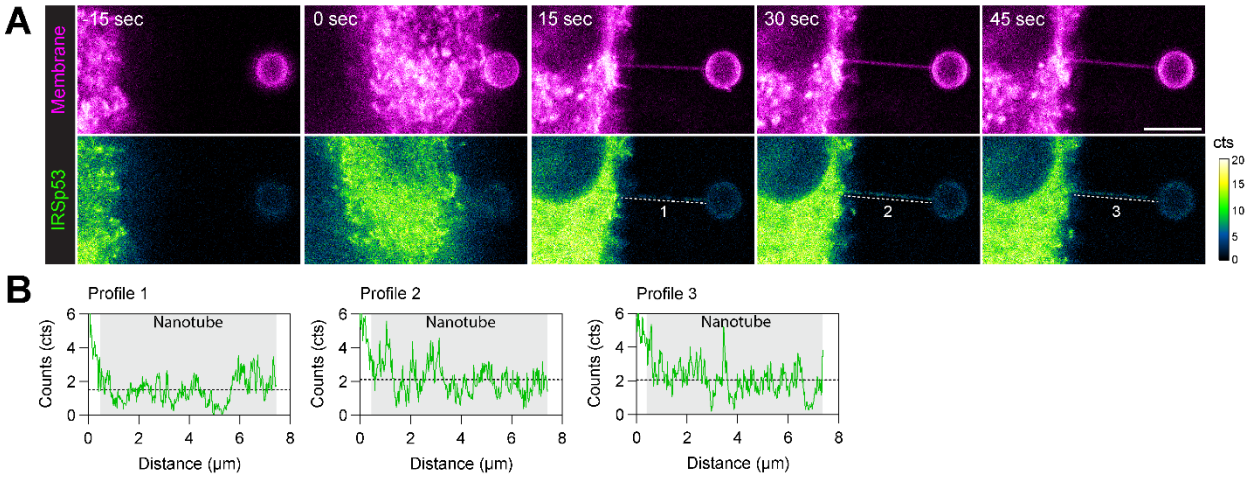

Fig. S16. IRSp53 rapidly equilibrates in nanotubes shortly after pulling.

(A) Confocal imaging during membrane nanotube pulling from an IRSp53-eGFP (green) expressing Rat2 cell. The plasma membrane was visualized using Cell Mask™ Deep Red stain (magenta). (B) Intensity profile plots of IRSp53 in the pulled nanotube. Profiles were measured along the nanotube from the base to the bead edge (dashed white lines in A) and the intensity was averaged over a given range (shaded gray region, 0.5 µm to the nanotube end). Average IRSp53 intensity values: Profile 1, 1.5 cts; Profile 2, 2.1 cts; 2.1 cts. Scale bar, 5 µm.

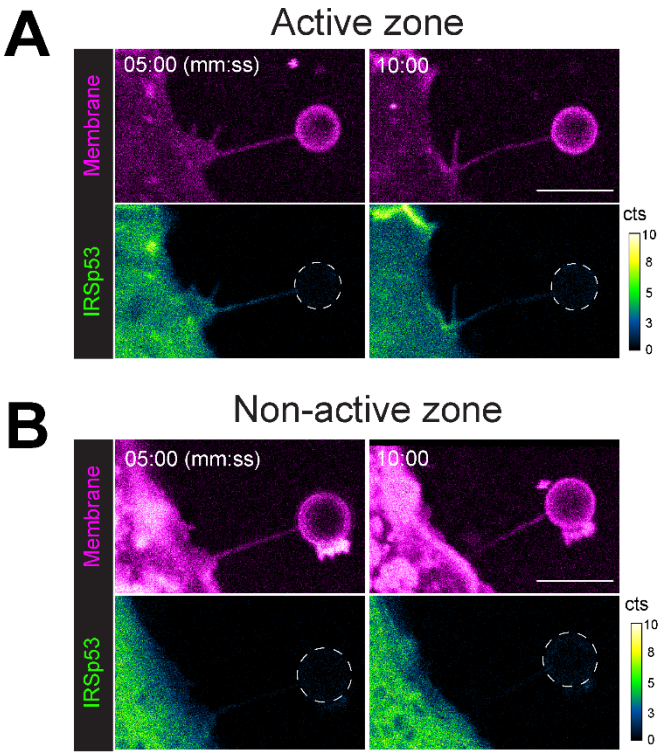

Fig. S17. Representative nanotubes pulled from "active" (A) and "non-active" zones (B) show that the presence or absence of IRSp53 FL, respectively, is stable through time.

Indicated times are defined from the point at which the nanotube was formed. Color codes: Cell Mask™ Deep Red (magenta), IRSp53-eGFP (green). Dashed white circles outline the trapped bead. Scale bars, 5 μm.

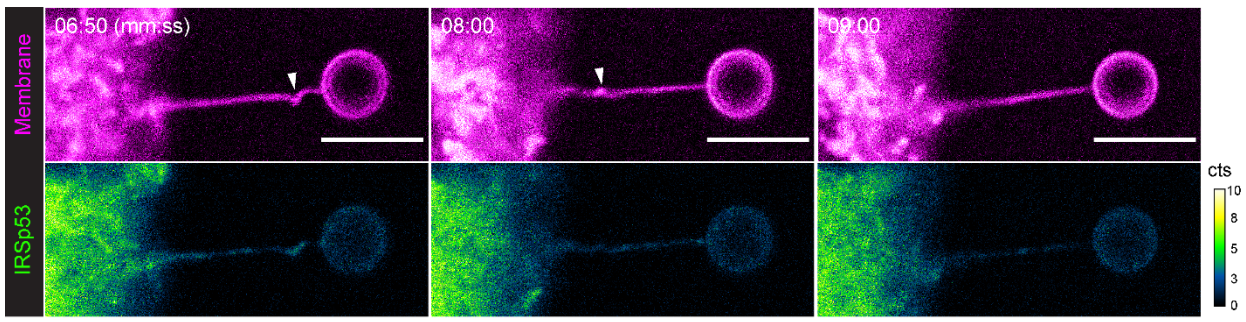

Fig. S18. Representative example of an IRSp53 positive nanotube exhibiting helical buckling (white arrowheads).

Indicated times are defined from the point at which the nanotube was formed. Color codes: Cell Mask™ Deep Red (magenta), IRSp53-eGFP (green). Scale bars, 5 μm.

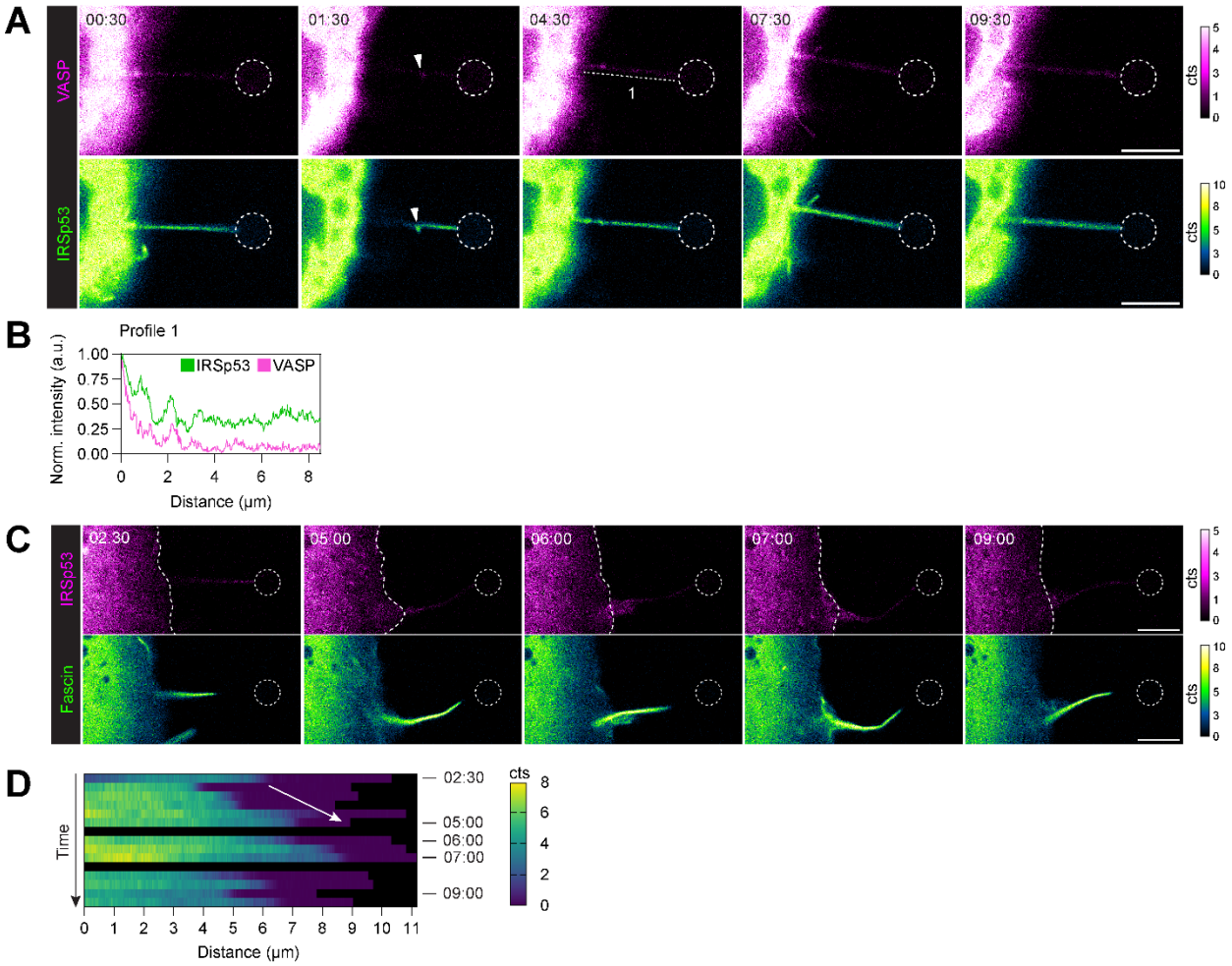

Fig. S19. VASP and fascin localize to IRSp53-positive nanotubes.

(A) Selected still images from Movie S10 showing a pulled nanotube positive for both RFP-VASP (magenta) and IRSp53-eGFP (green). Events of helical buckling are annotated with a white arrowhead. (B) Overlayed intensity profile plot of VASP and IRSp53. The profile was measured along the nanotube from the base to the bead edge (dashed white line in A) and normalized by the maximum intensity value. (C) Selected still images from Movie S11 showing a pulled nanotube positive for both IRSp53-mCherry (magenta) and eGFP-Fascin (green). (D) Kymograph of fascin fluorescence within the nanotube whose length was determined from the cell edge (dashed white lines in C) to the bead edge. The white arrow annotates fascin growth within the nanotube. Time in mm:ss. Dashed white circles in the figure outline the trapped bead. Scale bars, 5 μm.

Movie S1. IRSp53 clusters are followed by the birth of VASP clusters at the onset of a filopodium.

Live Rat2 cells expressing IRSp53-eGFP (green) and RFP-VASP (red). Time in seconds.

Movie S2. Aggregation of I-BAR domains in 2% PIP_2-like membrane

I-BAR domains are shown in red and PIP_2-like beads in blue.

Movie S3. Aggregation of I-BAR domains in 2% PIP_2-like membrane with only the center part of the I-BAR domains shown

The center part of the I-BAR domains is shown in yellow and PIP2-like beads in blue.

Movie S4. IRSp53 drives VASP-actin-based membrane protrusions.

Time-lapse imaging of a GUV exhibiting actin-filled membrane tubes. GUV membranes contained 0.5 mole% of BODIPY TR ceramide (magenta). A 10% - 27% of actin is tagged with AX488 (green). Time in mm:ss. Scale bar, 5 μm.

Movie S5. IRSp53 drives VASP-actin-based membrane protrusions.

Time-lapse imaging of a GUV exhibiting actin-filled membrane tubes. GUV membranes contained 0.5 mole% of BODIPY TR ceramide (magenta). A 10% - 27% of actin is tagged with AX488 (green). Time in mm:ss. Scale bar, 5 μm.

Movie S6. IRSp53 drives VASP-actin-based membrane protrusions.

Time-lapse imaging of a GUV exhibiting actin-filled membrane tubes. GUV membranes contained 0.5 mole% of BODIPY TR ceramide (magenta). AX488 phalloidin was used to visualize actin filaments (green). Time in mm:ss. Scale bar, 5 μm.

Movie S7. IRSp53 drives VASP-actin-based membrane protrusions.

Time-lapse imaging of a GUV exhibiting actin-filled membrane tubes. GUV membranes contained 0.5 mole% of BODIPY TR ceramide (magenta). AX488 phalloidin was used to visualize actin filaments (green). Time in mm:ss. Scale bar, 5 μm.

Movie S8. Recruitment of Fascin in IRSp53-induced filopodia.

Live Rat2 cells expressing IRSp53-eGFP (green) and mCherry-fascin (red). Time in seconds. Scale bar: 0.7 μm.

Movie S9. I-BAR-eGFP is enriched in nanotubes pulled from live cells.

Time-lapse imaging of a Rat2 cell expressing IRSp53's I-BAR domain fused to eGFP (green). Cell Mask™ Deep Red (magenta) was used to visualize the plasma membrane and the pulled nanotube. Imaging started 1 minute after the nanotube was formed. Time in mm:ss. Scale bar, 5 μm.

Movie S10. VASP localizes to IRSp53-positive nanotubes.

Time-lapse imaging of a Rat2 cell co-expressing IRSp53-eGFP (green) and RFP-VASP (magenta). Imaging started 30 sec after the nanotube was formed. The nanotube was refocused at frame 2 (00:30) and detached from the bead at frame 21 (10:00). Time in mm:ss. Scale bar, 5 μm.

Movie S11. Fascin localizes to IRSp53-positive nanotubes.

Time-lapse imaging of a Rat2 cell co-expressing eGFP-Fascin (green) and IRSp53-mCherry (magenta). Imaging commenced as the trapped bead was brought into cell contact to pull the nanotube. The pulled nanotube is focused into view at frame 5 (02:00). Time in mm:ss. Scale bar, 5 μm.